Materials Horizons

ROYAL SOCIETY OF CHEMISTRY

COMMUNICATION

View Article Online
View Journal

Cite this: DOI: 10.1039/d6mh00075d

Received 14th January 2026,
Accepted 24th March 2026

DOI: 10.1039/d6mh00075d

rsc.li/materials-horizons

A low interfacial-toughness self-segregating thermoset for large-scale ice-shedding coating application

David G. T. Boucher, [a] Jiayue Huang,[cd] Joseph Dahlgren,[a] Anish Tuteja [bcde] and Dean C. Webster *[a]

The accretion of ice is detrimental in numerous domains, and thus, developing ice-release coatings is of great significance. The recent introduction of stress-localized surfaces has opened new prospects in the development of ice-shedding coatings that could lead to more durable materials. However, the different ice-shedding solutions that have been developed so far lack durability or are too complex to be implemented successfully on an industrial scale. Therefore, we here investigate the potential of one-pot self-segregating siloxane–polyurethane (Si–PU) thermosets as durable stress localized surfaces for easy ice-shedding of large-scale icing. In this context, we explore the propensity of self-segregating Si–PU coatings to display surface modulus heterogeneities and the ability of such heterogeneities to initiate and propagate a crack at the ice/coating interface.

New concepts

Based on the concept of stress localization, we developed a one pot self-segregating siloxane polyurethane coating exploiting the formation of surface modulus heterogeneities to induce low interfacial toughness between ice and the coating's surface. Achieving interfacial toughness was found to be conditioned by the presence of domains at the interface, with the presence of domains solely in the bulk or of a PDMS layer at the surface being found to be insufficient to trigger low interfacial toughness. For the first time, the obtained material displayed low interfacial toughness while exhibiting a relatively elevated modulus (>1 GPa), without requiring the submicron thicknesses (here thickness ≥30 μm) typically reported in previous work and using an approach free of any complex engineering. This work provides significant insight into parameters influencing stress localization induced low interfacial toughness and opens the way, thanks to the high mechanical properties achieved through this approach (when opposed to the traditional silicone elastomers reported so far in this field), to the development of more durable and application friendly coatings to tackle large-scale icing issues.

Introduction

The accretion of ice onto structures has critical consequences in fields such as aeronautics,[1] energy transmission,[2] off-shore facilities,[3] marine vessels,[3] wind turbines,[4] and many others.[2] Among the proposed solutions, the application of silicone elastomers onto structures stands out due to their simplicity of application (requiring no specific surface topography), low surface energy, and low modulus.[5–10] Low surface energy helps minimize the interaction with water/ice,[7,10] while low modulus reduces the adhesion of solid objects onto the elastomer, as modeled by the Kendall law, often due to interfacial cavitation (surface buckling).[10–12] However, the low modulus of the elastomeric coating matrix is often synonymous with limited durability due to low mechanical properties.[13] In addition, for the interfacial slippage effect to be effective, the low modulus must be accompanied by a relatively large thickness of the soft material,[14,15] which increases the weight of the coating and its cost. Furthermore, silicone elastomers are also known for their poor adhesion towards many substrates (which leads to the need for a tie-coat or a specific treatment of the substrate) and are challenging to adapt for large-scale ice-shedding.[16–18]

Several alternatives to silicone elastomers have been explored, including textured surfaces and slippery liquid-infused porous surfaces, which have shown promising ice-shedding results. However, their complexity of implementation and low durability over multiple icing-deicing cycles often make their industrial application challenging.[19,20] A more promising and simpler alternative may be found in the use of heterogeneous but smooth surfaces, exploiting differences in foulant/surface bonding interactions along the interface to prevent a strong attachment.[21–25] The presence of heterogeneities in modulus, in particular, was found

[a] Department of Coatings and Polymeric Materials, North Dakota State University, Fargo, North Dakota, 58108, USA. E-mail: dean.webster@ndsu.edu
[b] Department of Materials Science and Engineering, University of Michigan, Ann Arbor, MI, 48109, USA
[c] Biointerfaces Institute, University of Michigan, Ann Arbor, MI, 48109, USA
[d] Department of Macromolecular Science and Engineering, University of Michigan, Ann Arbor, MI, 48109, USA
[e] Department of Chemical Engineering, University of Michigan, Ann Arbor, MI, 48109, USA

to be of interest to reduce the adhesion of ice onto surfaces.[13,26–31] For instance, He *et al.* incorporated micro-voids (air pockets) within a thin silicone material using a complex photolithography process.[26] The presence of these micro-voids created a different stiffness of the surface above the micro-void compared to above the bulk of the material, which then induced a "deformation mismatch" of the surface under stress, generating a crack at the ice/coating interface. Similarly, Ghasemi *et al.* dispersed soft PDMS microgels into a PDMS elastomer and reported a significantly lower ice adhesion than that for previously reported unmodified silicone elastomers.[13] This finding was attributed to a low force induced cracking of the ice/coating interface triggered by a localization of the stress at the interface between the heterogeneity and the ice. Using the same principle, Hure *et al.* provoked easy cracking of an ice/metal interface by creating microcavities and filling them with soft polymers such as silicones.[27] The concept of stress localized surface (SLS) appears to be equally applicable when including harder heterogeneities within a soft matrix. For instance, Zhang *et al.* incorporated hard PVC fillers into a soft PDMS elastomer to induce low ice adhesion.[28] However, good ice shedding of a large scale of icing was reached only using an additional plasticizer, which reduces the modulus and may leach out, thus impairing the long-term properties.

Although these systems exhibit promising properties, the requirement of multiple steps in their preparation, or the limited durability of soft PDMS, makes the practical implementation of such coatings challenging.[18,32] To resolve the durability issue, Ghasemi *et al.* incorporated PDMS microgels and silica particles into a PU matrix to form a network "guiding" the propagation of the crack.[33] Despite being one of the icephobic materials with the highest mechanical durability (Young's modulus as high as 10 GPa) reported to date, this material uses a multi-step preparation process that complicates any consideration of industrial large-scale application. Additionally, almost all the research cited above only focuses on the adhesion of small pieces of ice, an approach now considered insufficient to assess large scale performance,[34] as a loss of proportionality between force and the surface area [ice adhesion $(\tau_{ice}) = F/A$] was observed in many materials for large scales of icing.[35]

Hence, the present study aims to investigate the potential of one-pot self-segregating siloxane–urethane coatings[36–39] as durable and crack-propagation-initiating ice-shedding surfaces. We first examine the influence of the PDMS domains on the surface modulus and scrutinize the ice-shedding properties of the coatings. The objective is to determine if the presence of soft PDMS domains would trigger stress localization and crack propagation at the ice/coating interface, in turn, leading to low interfacial toughness coatings: a property that is crucial to facilitate large-scale ice shedding. Additionally, the influence of the domain size and the type of PDMS on the interfacial toughness is investigated. Finally, the durability of the presented coatings is demonstrated in terms of the bulk mechanical properties and conservation of the unique surface topography of the coating over time.

Results and discussion

Primary characterization of the coating surfaces

Self-segregating siloxane–urethane coatings were obtained either by co-reacting an IPDI-based polyisocyanate with a tri-functional hydroxy terminated polycaprolactone (Placcel 305) and a carbinol-difunctional PDMS [C-PDMS] or with an amino-functional PDMS [A-PDMS], as presented in Scheme 1. We named the samples as a function of the wt% of PDMS included in the formulation, the type of PDMS (A- or C-PDMS), and the time of mixing of the formulation before its application. Thus, the formulation containing 5% of C-PDMS and mixed for 4 h will be referred to as 5% C-PDMS-4 h. Formulation details are provided in the SI.

As previously reported, different surface topographies are obtained as a function of the amount of PDMS and the time allowed for the mixing step prior to application of the coating.[36–39] Such a variation of surface topography is depicted in Fig. 1 for samples obtained with C-PDMS. Smaller (microscopic) domains are obtained for lower PDMS content or longer mixing times, while larger, and even macroscopic, domains are obtained for higher PDMS content or shorter mixing times. The reduction in domain size with time of mixing is attributed to a higher extent of PDMS reacting with the IPDI polyisocyanate before application, thereby improving the interaction between the PU and PDMS phases and increasing the interfacial area between the two phases.

In this study, we selected seven self-segregating surfaces with different topographies and one PU control (0% PDMS, 4 h) to investigate their ice-shedding properties. The different surface morphologies of the coatings are presented in Fig. 2, which were mainly obtained by varying the amount of PDMS and the time of mixing, as well as the type of PDMS (C-PDMS *vs.* A-PDMS). AFM surface topography and roughness data were also recorded and

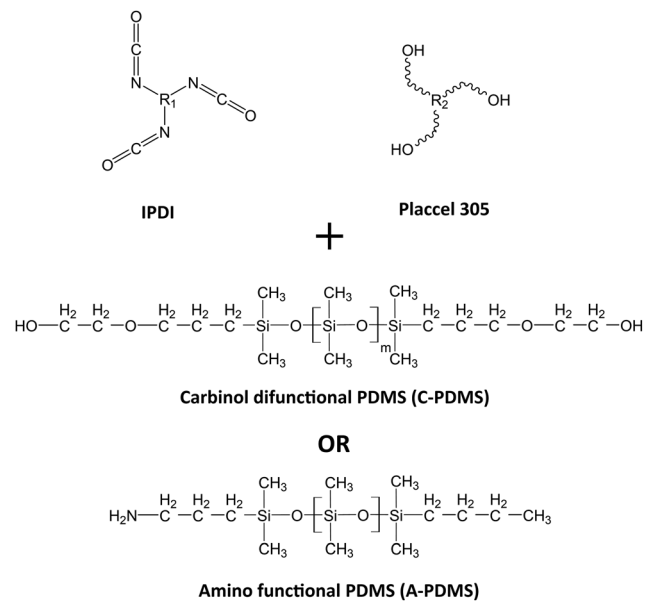

Scheme 1 Structure of the components entering the self-segregating coating formulation.

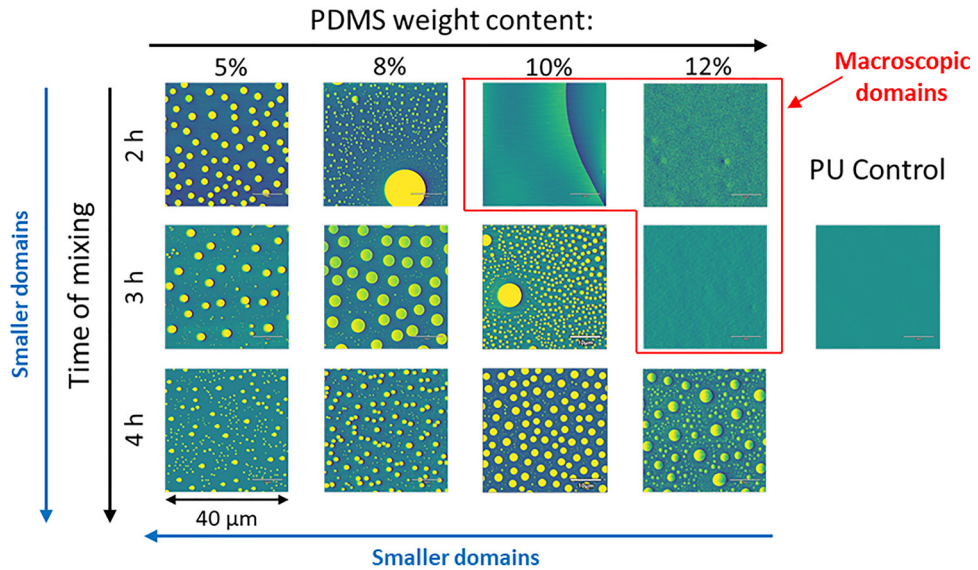

Fig. 1 AFM phase imaging of the coating surfaces as a function of C-PDMS content and time of mixing.

are reported in Fig. S1 and Table S3. As the presence of domains may be difficult to see in the image presented in Fig. 2 for 5% A-PDMS-4 h, we also provided smaller scan sizes in Fig. S1, highlighting the presence of nanometric domains for this surface.

Through AFM analysis of the surface, we determined that the 5% A-PDMS-O sample (the only sample where the amino-functional PDMS was pre-reacted with the isocyanate before mixing it with the polyol) was the only surface, along with the PU control, that did not have discrete domains on the surface. However, optical microscopy images obtained during the AFM experiment (Fig. S2) clearly show domains in the bulk of 5% A-PDMS-O, as is the case for all of the PDMS-containing samples. The presence of domains within the bulk of the coatings was further confirmed by SEM and TEM analyses of coating cross-sections (Fig. S3). These observations indicate that the formation of these domains is likely induced by emulsion-like phase segregation during the mixing process and highlight that 5% A-PDMS-O is the only sample of the set to present domains within its bulk but not on its surface.

We verified the PDMS nature of the domains visible at the surface of the coatings by Pi-FM analysis, as shown in Fig. S4, and found that the presence of PDMS at the surface was consistent with the measured surface energies for the coatings.

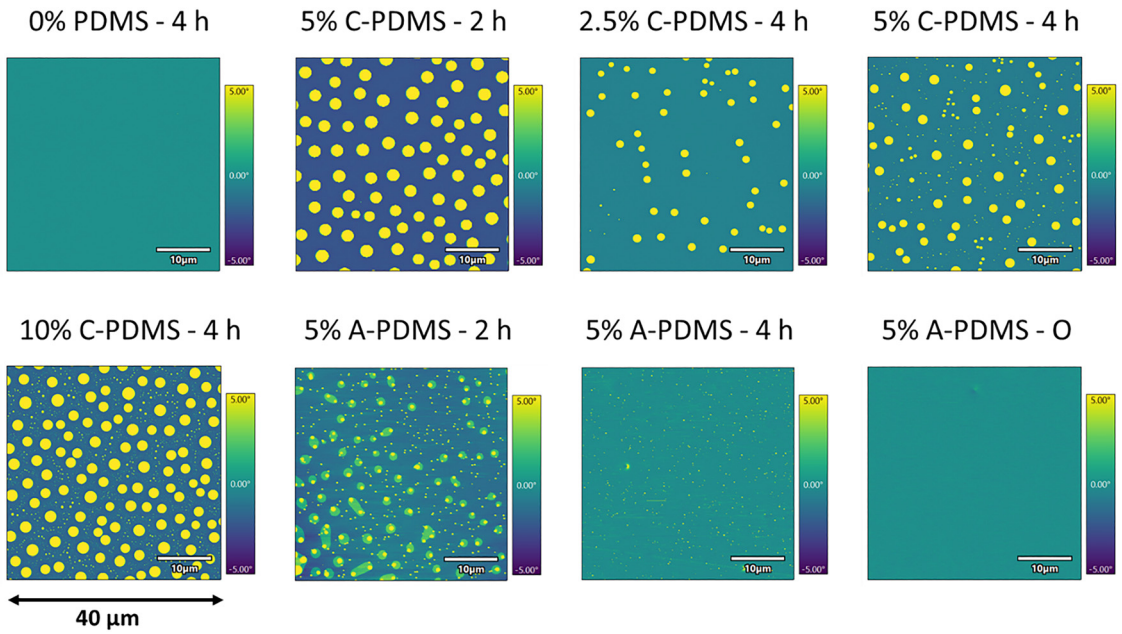

Fig. 2 AFM phase imaging of the coating surfaces investigated in this study.

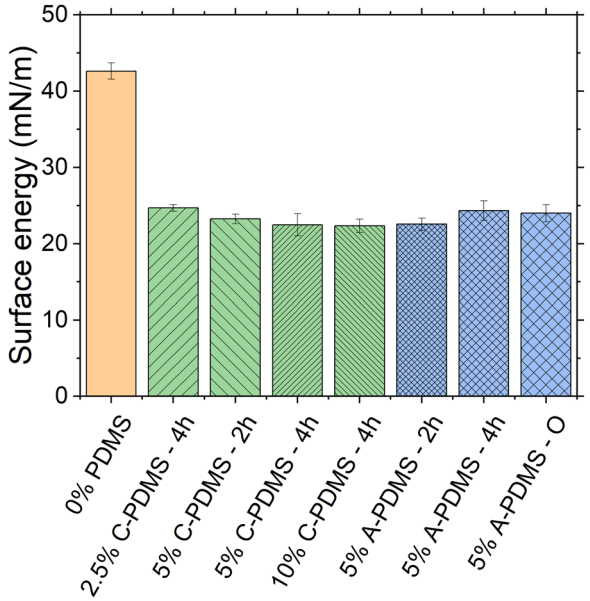

Fig. 3 Surface energies determined from water and diiodomethane contact angles.

All PDMS-containing coatings presented a surface energy of approximately 22.5 mN m^{-1} (Fig. 3), corresponding to the value typically expected for a PDMS material (22–25 mN m^{-1})[40,41] and indicating that the surface energy of the surface is primarily governed by the presence of the PDMS microdomains. Although no domains were observed at its surface, the sample 5% A-PDMS-O also presented a PDMS-like surface energy, indicating that the surface is covered by a homogeneous layer of PDMS.

Finally, we performed AFM force mapping to evaluate if the presence of these domains on the surface led to significant (over one order of magnitude) modulus variations on the surface of the coatings (Fig. 4). Note that given the experimental conditions, we do not consider the absolute values of modulus to be reliable as such and rather focus here on the observation of significant variations of modulus felt on the surface, which we consider to indicate the presence of harder and softer segments. As postulated earlier, the modulus of the PDMS domains was found to be about 1 to 2 orders of magnitude ($\approx$50 to 100 MPa) below the one of the surrounding polyurethane matrix ($\approx$1 GPa), indicating an overall high modulus surface (polyurethane) containing distributed soft PDMS 'pockets.' Interestingly, the presence of softer domains was highlighted in each of the PDMS-containing samples, with the exception of the sample 5% A-PDMS-O, which did not display PDMS domains on its surface, further confirming that the variations of modulus observed are induced by the presence of the PDMS domains at the surface and not in the bulk.

Ice shedding properties and impact of PDMS domains' size and coverage

To determine if the measured modulus heterogeneities could translate into advantageous ice-shedding properties, we investigated the adhesion of pieces of ice of 1 cm width, 0.6 cm height, and length varying from 1 to 14 cm. All samples displayed an initial linear increase in force necessary to remove the ice as the size of ice increased (Fig. 5); however, the self-segregating C-PDMS coatings and some A-PDMS coatings displayed a constant force above 6–8 cm. This transition from a linear increase to a plateau was previously described as the transition from a strength-controlled to a toughness-controlled regime, where the force becomes independent of the surface area of the interface.[35] The interfacial toughness between two materials corresponds to the resistance of their interface to the propagation of a crack; thus, materials with low interfacial toughness towards ice are preferable to mitigate large-scale ice accretion due to the ease of crack propagation between the two materials.[35] The difference in behavior observed between the PU control and the self-segregating coatings is attributed to the presence of the PDMS microdomains at the surface of the coatings. The impact of surface heterogeneities is all the more striking since the 5% A-PDMS-O sample, being the only sample showing no surface domains, is the only experimental coating to not present a plateau of force. One could argue that the formation of a PDMS layer on the surface of 5% A-PDMS-O could modify the distribution of stress on the surface and may negatively influence the presence of a plateau of force. However, Golovin *et al.* previously demonstrated that soft and thin (micron sized) surface layers such as PDMS actually favor the attainment of a low interfacial toughness plateau.[35] We may only assume here that the difference between our result with our 5% A-PDMS-O and Golovin's can be ascribed to the submicron size of the PDMS layer (most likely a few atoms) which makes the mechanical properties of the PDMS layer negligible. This assumption is consistent with the absence of difference in the surface modulus felt by AFM on 5% A-PDMS-O and 5% A-PDMS-4 h outside of the PDMS domains. Moreover, these observations also highlight that a simple decrease of surface energy (due to the presence of a PDMS layer) is not sufficient to trigger a plateau of force.

Given the previous work performed on the localization of stresses by creating macro-voids or by introducing PDMS microgels into a PDMS matrix,[13,42] we mostly assumed that the presence of two significantly distinct moduli at the surface of a material may lead to a heterogeneous deformation response across the surface, inducing a concentration of the applied stress in specific areas, thus facilitating the initiation and propagation of a crack. However, one should also consider that, as a strong icephobic material (has low interaction with ice),[35] the presence of PDMS microdomains at the interface could also create weak points in the bonding of ice/coating, likely to initiate cracks and facilitate their propagation as previously suggested in the case of amphiphilic materials.[25] At the moment, since the PDMS additive and the polyurethane present both different moduli and interactions with ice, it is unfortunately impossible for us to determine exactly which of these factors are predominant in the observation of low interfacial toughness, and we can only assume that both factors may have a concerted effect. To obtain more insight into the specific contribution of each factor, future work should involve the

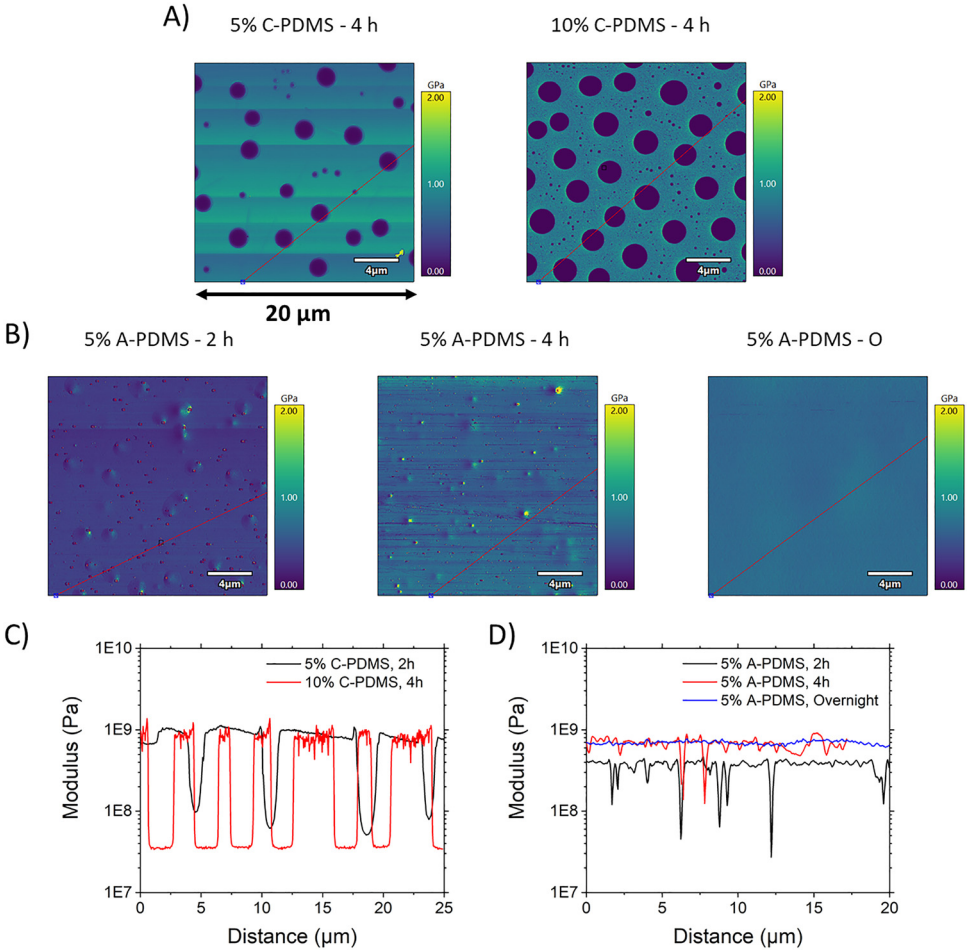

Fig. 4 (A) Force mapping analysis of C-PDMS samples. (B) Force mapping analysis of A-PDMS samples. (C) Variation of the modulus along the red lines traced in (A). (D) Variation of the modulus along the red lines traced in (B).

design of similar coatings presenting, this time, heterogeneities solely in modulus or surface energy on their surfaces.

We calculated the interfacial toughness values from the critical force (average of the forces on the plateau) using the following equation described in previous work:[35]

$$\text{Interfacial toughness } (\Gamma) = \frac{(F_c)^2}{2E_{ice}h}$$

where F_c corresponds to the critical force (force recorded on the plateau), E_{ice} to the modulus of ice (8.5 GPa) and h to the thickness of ice. We report values of interfacial toughness in Table 1 along with the critical force and τ_{ice} (ice adhesion from the strength control regime). A strict consideration of these absolute values for the C-PDMS family would suggest that the 5% C-PDMS-4 h coating is the best performing self-segregating coating and the 5% C-PDMS-2 h is the worst performing one. However, tracing all of the force curves on a unique graph (Fig. S5) highlights a superimposition of almost all of the data points obtained for the self-segregating samples, with the exception of two outliers that lower the average critical force of 5% PDMS-4 h and increase the forces for 5% PDMS-2 h, respectively. We thus consider that the interfacial toughness of the self-segregating coatings is not impacted by the size of the domains and their coverage on the surface, at least within the ranges tested in this study.

In a similar fashion, and despite the significant difference in domain sizes, 5% A-PDMS-2 h and 5% A-PDMS-4 h showed no difference in critical force, further highlighting the limited impact of the domain size. We also found the values of τ_{ice} obtained for the A-PDMS samples to be similar to the ones of the C-PDMS or PU control samples, while the critical force ($\approx$72 N cm^{-1}) and interfacial toughness ($\Gamma \approx 0.52$ J m^{-2}) were slightly lower than those obtained for the C-PDMS (about 85 N cm^{-1} and 0.70 J m^{-2}). This tendency suggests that the mono-functional A-PDMS tends to yield slightly better performing ice-releasing surfaces, even though it is not clear (at the moment) if this difference is induced by its lower number of functional end groups (1 functional end of chain *vs.* 2 for C-PDMS), its higher molar mass (2000 g mol^{-1} *vs.* 1000 g mol^{-1} for C-PDMS), or its functionality (amine *vs.* carbinol).

We finally compared the force curves of a 5% A-PDMS-4 h coating of either 80 or 30 μm thickness to determine the thickness effect on ice release (Fig. 6). Although we did not observe any significant change in τ_{ice} between the two coatings,

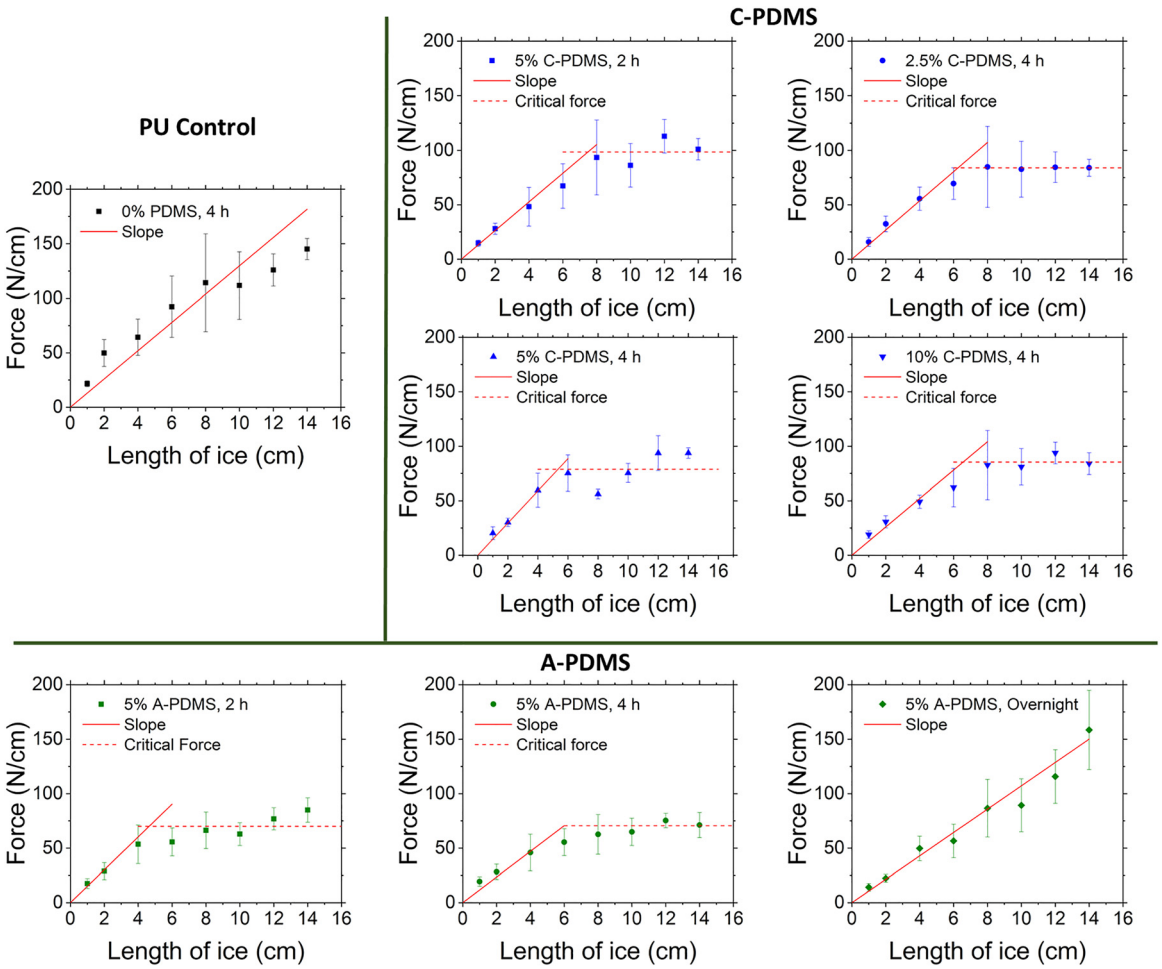

Fig. 5 Force (expressed per unit of width) recorded for the removal of ice samples from the surfaces as a function of the length of the ice. All coatings are between 80 and 100 μm thick.

Table 1 Coating properties as a function of PDMS content and time of mixing

Sample	% PDMS	Mixing time (h)	Thickness (μm)	τ_{ice} (kPa)	Critical force (N cm^{-1})	Interfacial toughness (J m^{-2})
PU control	0	4	85 ± 10	130 ± 17	Not reached	Not reached
C-PDMS	2.5	4	80 ± 10	134 ± 10	84.0	0.69 ± 0.35
	5	2	100 ± 10	132 ± 7	98.5	0.95 ± 0.38
	5	4	80 ± 10	148 ± 10	78.5	0.61 ± 0.16
	10	4	90 ± 10	130 ± 13	85.4	0.72 ± 0.29
A-PDMS	5	2	80 ± 10	150 ± 12	74.9	0.55 ± 0.16
	5	4	75 ± 5	118 ± 20	70.5	0.49 ± 0.14
	5	4	30 ± 5	144 ± 21	50.9	0.25 ± 0.10
	5	Overnight	80 ± 15	107 ± 5	Not reached	Not reached

we found a decrease in critical force to about 50 N ($\Gamma \sim 0.25$ J m^{-2}) as the thickness of the coating was decreased to 30 μm. This decrease agrees with previous observations and theoretical considerations[35] and highlights the possibility of reaching interfacial toughness properties very close to the theoretical limit of 0.1 J m^{-2} by reducing the thickness even further.[35] The same experiment was not performed on the C-PDMS series due to the significant number of defects on the surface of 30 μm coatings, which may be ascribed to the absence of surface treatment of the substrate (wetting issue).

Durability

Since we expressed, in the Introduction, the need for durable coatings for ice-shedding, we investigated the durability of our coatings by testing the impact of the PDMS domains on Young's modulus and abrasion resistance (Fig. 7). Overall, Young's modulus of the coatings was not significantly affected by the addition of PDMS, with a measured minimum of 1.38 GPa *vs.* 1.60 GPa for the PU control. The coatings of the C-PDMS series appear to present slightly higher modulus than the A-PDMS series (ranging from 1.38 to 1.54 GPa), which we

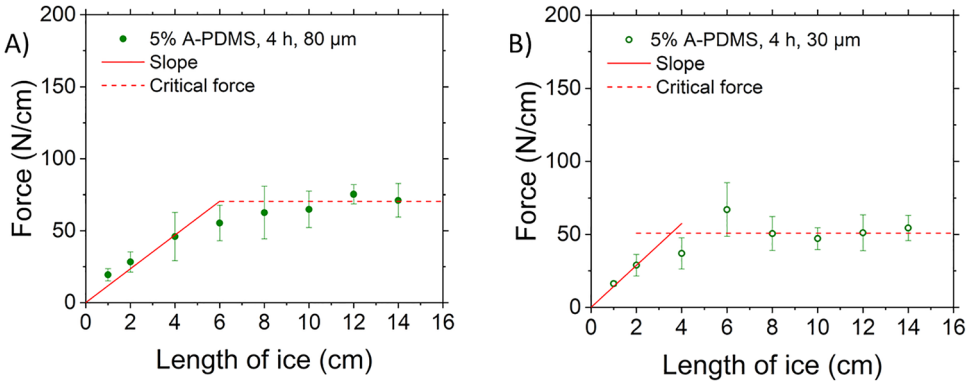

Fig. 6 Comparison of the force (expressed by unit of width) curves obtained as a function of ice length for a 5% A-PDMS formulation of samples with a thickness of 80 (A) or 30 µm (B).

ascribe to the mono-functionality of A-PDMS, leading to the presence of dangling polymer chains in the network. Additionally, Young's modulus of A-PDMS seems to be affected by the time of mixing, which is likely due to an increase of the amount of PDMS chains that reacted with isocyanate and integrated into the network over time. By Taber abrasion, we observed an increase of approximately 15 mg/1000 cycles in the wear index when adding PDMS to the formulation. However, this difference is within the standard deviation range observed for the PU control. Moreover, ASTM D4060-19 (Taber abrasion standard) indicates an expected wear index of approximately 50 mg/1000 cycles for PU coatings, implying that our PDMS-modified coatings behave as well as any PU coatings, with a weight loss observed within tens of milligrams, indicating fairly robust coatings.

To further highlight the difference in mechanical properties between the coatings presented in this study and the materials usually reported in the ice-shedding field, we would like to underline that the modulus of a typical PDMS material ranges between 100 kPa and 1–5 MPa,[43–45] a significantly lower value than the minimum value of 1.38 GPa obtained in our study. Moreover, Golovin *et al.* showed that extremely low interfacial toughness could only be achieved with extremely thin (1.5 µm) PDMS coatings (while thicker PDMS coatings yield lower τ_{ice} values), while materials presenting higher mechanical properties (modulus > 0.5 GPa) did not provide low interfacial toughness, even at equivalently low thicknesses.[35] To bring low interfacial toughness to a PVC material, Golovin *et al.* highlighted the need to significantly reduce its modulus (from 3.6 GPa to 120 MPa, about 97% decrease) by adding 50 wt% of medium-chain triglyceride oil as a plasticizer and to produce extremely thin (1 µm) coatings.[35] Later, low interfacial toughness was reached for thicker (50 µm) PVC coatings by adding even more plasticizer (60 wt%).[46] However, such an approach is likely to decrease even further the modulus of the matrix and to negatively affect the durability of the properties due to the overtime depletion of the plasticizer. In comparison, the method proposed in our study does not significantly reduce the modulus of the coating (minimum of 1.38 GPa against a value of 1.60 GPa for the PU control), does not require the use of a non-bonded additive, and does not require an extremely low coating thickness of 1–2 µm (uncommon for organic coatings). The developed coatings thus demonstrate a higher tolerance to thickness variations of a few microns during the application process, as well as improved overall coating durability. Fig. 8

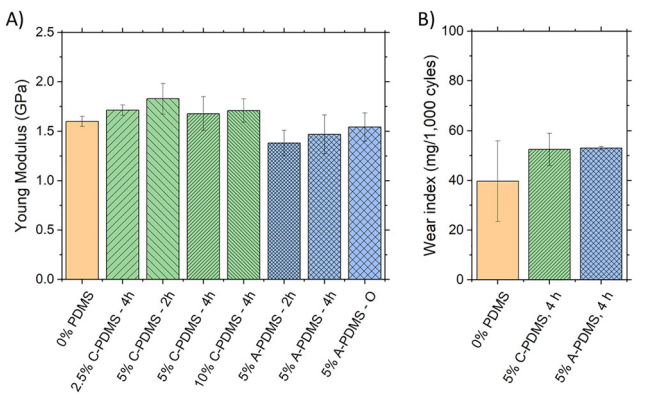

Fig. 7 (A) Young's modulus measured through the tensile test. (B) Weight losses observed during Taber abrasion experiments, using a CS-10 grit.

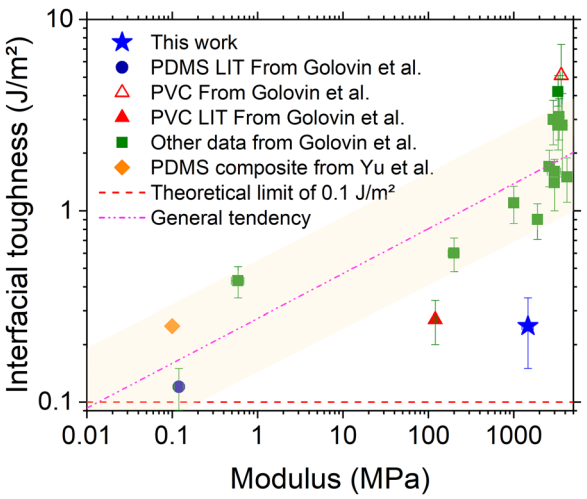

Fig. 8 Graphical comparison of the interfacial toughness and modulus of the best coating of our work (5% A-PDMS-4 h, 30 µm) and the ones of the materials investigated by Golovin *et al.*[35] or Yu *et al.*[47]

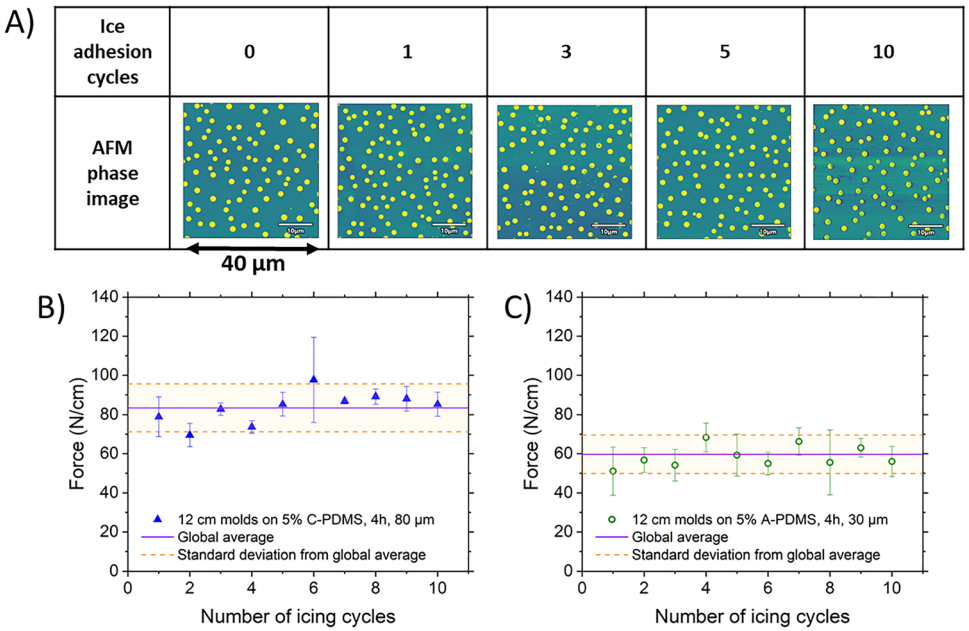

Fig. 9 (A) AFM phase images obtained in between icing/push-off cycles on the sample 5% C-PDMS-4 h, 80 µm thick. (B) Ice adhesion measured over 10 icing/push-off cycles using a 12 cm mold on the sample 5% C-PDMS-4 h, 80 µm thick. (C) Force measured on the plateau over 10 icing/push-off cycles using a 12 cm mold on the sample 5% A-PDMS-4 h, 30 µm thick.

presents a graphical comparison between the interfacial toughness and modulus values reported in this work and those reported in previous publications.

We performed 10 icing/push-off cycles on 5% C-PDMS-4 h and performed AFM analysis of the tested surface in between icing/push-off cycles while ensuring to test the exactly same surface over and over by marking it. Fig. 9A shows no obvious degradation or deformation of the surface over 10 cycles. Additionally, the values obtained for the removal of a 12 cm mold (on the plateau of force) appear to be fairly stable over the 10 cycles, as shown in Fig. 9B. Similarly, our lowest interfacial toughness formulation (5% A-PDMS-4 h and 30 µm thick) highlighted a strong stability of the value found on the plateau over the 10 icing/push-off cycles (Fig. 9C). No AFM imaging before/after was performed for this formulation due to the very small size of the domains.

Finally, we assessed a 5B adhesion ranking (0 being the lowest adhesion ranking and 5B the highest) for all formulations using the cross-hatch adhesion test method, ASTM D3359, when samples were coated over sandblasted aluminum. This result indicates good adhesion of the coating on the substrate, which we attributed to the absence of PDMS at the interface with the substrate (see the SI).

Transparency of the coatings

The transparency of coatings can be an important parameter for solar panels or light detectors used in areas subjected to freezing conditions. We thus roughly assessed the transparency of our coatings simply by peeling them off bare aluminum and placing them over the text as presented in Fig. 10. C-PDMS coatings appear to be almost as transparent as the PU control, with a clear distinction between the text and background colors. We thus

Fig. 10 Transparency of the PU control (0% PDMS, 4 h), compared to that of the self-segregating formulations (all coatings are about 80 to 100 µm thick).

expect these coatings not to disturb the passing of light and to be of potential interest for solar panels. A-PDMS coatings, however, displayed a much more pronounced haziness with a background color barely recognizable (due to the white aspect of the film), but still displayed a good definition of the text. To determine the applicability of these coatings for light-sensitive applications, additional investigation, such as optical transmission spectroscopy, would be necessary. However, as with the ice shedding properties, we expect the transparency of these coatings to be improved as their thickness is reduced from 80 to 30 μm.

Conclusions

In this study, we described the strong potential of one-pot self-segregating coatings in the field of ice-shedding coatings. We demonstrated that the siloxane–polyurethane (Si–PU) coatings investigated in this study exhibited PDMS micro-domains on their surface, which induced both modulus heterogeneities of over an order of magnitude and surface energy (icephobic/hydrophobic) heterogeneities, across the coating surface. Despite the presence of these domains (or modulus/surface energy heterogeneity), we did not observe any difference in ice adhesion strength (τ_{ice}) between the Si–PU coatings and the PU control. However, the presence of these domains at the surface did lead to the occurrence of a critical force for larger pieces of ice, which was not observed for the PU control or the one Si–PU coating of the study that did not present domains at its surface. The presence of this plateau of force only when heterogeneities are displayed on the surface highlights the benefit of such heterogeneities in producing a large-scale ice-shedding material. We found this critical force to be dependent, in addition to the presence of micro-domains, on the type of PDMS and the thickness of the coating, but to be independent of the relative size of the microdomains. We found that all Si–PU samples presenting surface heterogeneity displayed low interfacial toughness, with recorded values as low as 0.25 J m^{-2}, which is quite close to the theoretical lower limit of 0.1 J m^{-2}.[35] Such low interfacial toughness values were reached without requiring ultra-thin coatings (1–2 μm) but still necessitates relatively thin coatings (<100 μm), with the best performances reached as the coating gets thinner. More importantly, low interfacial toughness was reached without significant deterioration of the bulk mechanical properties, as demonstrated by the negligible decrease in Young's modulus and abrasion resistance upon addition of PDMS. Furthermore, the domains present on the surface, along with shedding properties, were found to be resilient over multiple icing/push-off cycles, suggesting (along with elevated Young's modulus) long-term durability and efficiency of the coatings. Finally, as an additional benefit, the transparency of some of the tested coatings makes their use in applications that require light transmission plausible.

Author contributions

David Boucher: conceptualization, investigation, methodology, validation, visualization, and writing – original draft; Jiayue Huang: conceptualization and investigation; Joseph Dahlgren: investigation; Anish Tuteja: conceptualization, funding acquisition, supervision, and writing – review and editing; Dean C. Webster: conceptualization, funding acquisition, project administration, supervision, and writing – review and editing.

Conflicts of interest

The authors declare no conflicts of interest.

Data availability

The data that support the findings of this study are available from the corresponding author upon reasonable request.

Supplementary information (SI), containing details of the experimental procedures and formulations as well as a few experimental results, is available. See DOI: https://doi.org/10.1039/d6mh00075d.

Acknowledgements

The authors thank the NDSU Electron Microscopy Core for providing us with the SEM and TEM images presented in this paper. This material is based upon the work supported by the National Science Foundation under grant no. 0821655.

This investigation was supported by the U.S. Navy's Office of Naval Research through grant nos. N00014-20-1-2817 and N00014-22-1-2129.

References

1 M. Bragg, T. Hutchison and J. Merret, Effect of ice accretion on aircraft flight dynamics. in *38th Aerospace Sciences Meeting and Exhibit*, American Institute of Aeronautics and Astronautics, 2000, DOI: 10.2514/6.2000-360.
2 K. F. Jones, Ice accretion in freezing rain, CRREL Rep. 96-2 31, 1996.
3 S. Mintu and D. Molyneux, Ice accretion for ships and offshore structures. Part 2 – Compilation of data, *Ocean Eng.*, 2022, **248**, 110638, DOI: 10.1016/j.oceaneng.2022.110638.
4 L. Makkonen, T. Laakso, M. Marjaniemi and K. J. Finstad, Modelling and prevention of ice accretion on wind turbines, *Wind Eng.*, 2001, **25**, 3–21, DOI: 10.1260/0309524011495791.
5 Y. Shen, X. Wu, J. Tao, C. Zhu, Y. Lai and Z. Chen, Icephobic materials: Fundamentals, performance evaluation, and applications, *Prog. Mater. Sci.*, 2019, **103**, 509–557, DOI: 10.1016/j.pmatsci.2019.03.004.
6 R. Menini and M. Farzaneh, Advanced Icephobic Coatings, *J. Adhes. Sci. Technol.*, 2011, **25**, 971–992, DOI: 10.1163/016942410X533372.
7 D. H. Berry and C. J. Wohl, Contamination Mitigating Polymeric Coatings for Extreme Environments, Advances in Polymer Sciences, 2018, vol. 284, DOI: 10.1007/978-3-030-45839-3.
8 Y. Zhuo, S. Xiao, A. Amirfazli, J. He and Z. Zhang, Polysiloxane as icephobic materials – The past, present and the

future, *Chem. Eng. J.*, 2021, **405**, 127088, DOI: 10.1016/j.cej.2020.127088.
9 E. M. Yorkgitis and K. C. Melancon, *Ice release composition, article and method*, *European Patent*, 0384597 A1, 1990.
10 Y. Liu, Y. Wu, S. Liu and F. Zhou, Material Strategies for Ice Accretion Prevention and Easy Removal, *ACS Mater. Lett.*, 2022, **4**, 246–262, DOI: 10.1021/acsmaterialslett.1c00365.
11 B. Z. Newby, M. K. Chaudhury and H. R. Brown, Macroscopic Evidence of the Effect of Interfacial Slippage on Adhesion, *Science*, 1995, **269**, 1407–1409, DOI: 10.1126/science.269.5229.1407.
12 M. K. Chaudhury and K. H. Kim, Shear-induced adhesive failure of a rigid slab in contact with a thin confined film, *Eur. Phys. J. E: Soft Matter Biol. Phys.*, 2007, **23**, 175–183, DOI: 10.1140/epje/i2007-10171-x.
13 P. Irajizad, A. Al-Bayati, B. Eslami, T. Shafquat, M. Nazari, P. Jafari, V. Kashyap, A. Masoudi, D. Araya and H. Ghasemi, Stress-localized durable icephobic surfaces, *Mater. Horiz.*, 2019, **6**, 758–766, DOI: 10.1039/C8MH01291A.
14 C. Wang, T. Fuller, W. Zhang and K. J. Wynne, Thickness dependence of ice removal stress for a polydimethylsiloxane nanocomposite: Sylgard 184, *Langmuir*, 2014, **30**, 12819–12826, DOI: 10.1021/la5030444.
15 C. Wang, M. C. Gupta, Y. H. Yeong and K. J. Wynne, Factors affecting the adhesion of ice to polymer substrates, *J. Appl. Polym. Sci.*, 2018, **135**, 45734, DOI: 10.1002/app.45734.
16 M. Lejars, A. Margaillan and C. Bressy, Fouling release coatings: A nontoxic alternative to biocidal antifouling coatings, *Chem. Rev.*, 2012, **112**, 4347–4390, DOI: 10.1021/cr200350v.
17 R. Mason and J. T. Koberstein, Adhesion of PDMS Elastomers to Functional Substrates, *J. Adhes.*, 2005, **81**, 765–789, DOI: 10.1080/00218460500188838.
18 M. Mohseni, Z. A. Dijvejin and K. Golovin, Designing scalable elastomeric anti-fouling coatings: Shear strain dissipation via interfacial cavitation, *J. Colloid Interface Sci.*, 2021, **589**, 556–567, DOI: 10.1016/j.jcis.2021.01.019.
19 Y. Zhuo, T. Li, F. Wang, V. Håkonsen, S. Xiao, J. He and Z. Zhang, An ultra-durable icephobic coating by a molecular pulley, *Soft Matter*, 2019, **15**, 3607–3611, DOI: 10.1039/c9sm00162j.
20 Z. He, Y. Zhuo, Z. Zhang and J. He, Design of icephobic surfaces by lowering ice adhesion strength: A mini review, *Coatings*, 2021, **11**, 1–26, DOI: 10.3390/coatings11111343.
21 V. Upadhyay, T. Galhenage, D. Battocchi and D. Webster, Amphiphilic icephobic coatings, *Prog. Org. Coat.*, 2017, **112**, 191–199, DOI: 10.1016/j.porgcoat.2017.07.019.
22 D. Chen, M. D. Gelenter, M. Hong, R. E. Cohen and G. H. McKinley, Icephobic Surfaces Induced by Interfacial Nonfrozen Water, *ACS Appl. Mater. Interfaces*, 2017, **9**, 4202–4214, DOI: 10.1021/acsami.6b13773.
23 J. S. Zigmond, K. A. Pollack, S. Smedley, J. E. Raymond, L. A. Link, A. Pavía-Sanders, M. A. Hickner and K. L. Wooley, Investigation of intricate, amphiphilic crosslinked hyperbranched fluoropolymers as anti-icing coatings for extreme environments, *J. Polym. Sci., Part A: Polym. Chem.*, 2016, **54**, 238–244, DOI: 10.1002/pola.27800.
24 B. Liu, K. Zhang, C. Tao, Y. Zhao, X. Li, K. Zhu and X. Yuan, Strategies for anti-icing: Low surface energy or liquid-infused?, *RSC Adv.*, 2016, **6**, 70251–70260, DOI: 10.1039/c6ra11383d.
25 A. G. Nurioglu, A. C. C. Esteves and G. De With, Non-toxic, non-biocide-release antifouling coatings based on molecular structure design for marine applications, *J. Mater. Chem. B*, 2015, **3**, 6547–6570, DOI: 10.1039/c5tb00232j.
26 Z. He, S. Xiao, H. Gao, J. He and Z. Zhang, Multiscale crack initiator promoted super-low ice adhesion surfaces, *Soft Matter*, 2017, **13**, 6562–6568, DOI: 10.1039/c7sm01511a.
27 H. Martin, J. Garcia and P. Olivier, *Article pour une application antigivre*, *French Patent*, 3125981, 2021.
28 P. Wang, M. Yang, B. Zheng, X. Guan, Y. Liao, Y. Yue, W. Duan and Y. Zhang, Soft and Rigid Integrated Durable Coating for Large-Scale Deicing, *Langmuir*, 2023, **39**, 403–410, DOI: 10.1021/acs.langmuir.2c02612.
29 T. Zhu, Y. Yuan, L. Song, X. Wei, H. Xiang, X. Dai, X. Hua and R. Liao, A PDMS coating with excellent durability for large-scale deicing, *J. Mater. Res. Technol.*, 2024, **29**, 4526–4536, DOI: 10.1016/j.jmrt.2024.02.177.
30 T. Zhu, Y. Yuan, X. Wei, X. Hua, X. Dai, H. Xiang, L. Song and R. Liao, Durable Low-Interfacial Toughness PDMS/SiO2 Coatings with Superior Anti-Icing and Large-Scale Deicing Performance in the Natural Field, *Adv. Mater. Interfaces*, 2025, **12**(16), 2500206, DOI: 10.1002/admi.202500206.
31 X. Sun, Y. Guo, C. Fang, C. Xu, Z. Zhang, Y. Zhu and L. Jiang, Modulus Mismatch-Guided Interlocked Microphase Separation for Fracture-Responsive Deicing in Ultraslippery Coatings, *ACS Appl. Mater. Interfaces*, 2025, **17**(48), 65862–65876, DOI: 10.1021/acsami.5c17002.
32 Y. Zhuo, J. Chen, S. Xiao, T. Li, F. Wang, J. He and Z. Zhang, Gels as emerging anti-icing materials: A mini review, *Mater. Horiz.*, 2021, **8**, 3266–3280, DOI: 10.1039/d1mh00910a.
33 S. Nazifi, Z. Huang, A. Hakimian and H. Ghasemi, Fracture-controlled surfaces as extremely durable ice-shedding materials, *Mater. Horiz.*, 2022, **9**, 2524–2532, DOI: 10.1039/d2mh00619g.
34 L. Stendardo, G. Gastaldo, M. Budinger, I. Tagliaro, V. Pommier-Budinger and C. Antonini, Why the adhesion strength is not enough to assess ice adhesion on surfaces, *Appl. Surf. Sci.*, 2024, **672**, 160740, DOI: 10.1016/j.apsusc.2024.160740.
35 K. Golovin, A. Dhyani, M. D. Thouless and A. Tuteja, Low–interfacial toughness materials for effective large-scale deicing, *Science*, 2019, **364**, 371–375, DOI: 10.1126/science.aav1266.
36 P. Majumdar and D. C. Webster, Preparation of siloxane-urethane coatings having spontaneously formed stable biphasic microtopograpical surfaces, *Macromolecules*, 2005, **38**, 5857–5859, DOI: 10.1021/ma050967t.
37 P. Majumdar and D. C. Webster, Influence of solvent composition and degree of reaction on the formation of surface microtopography in a thermoset siloxane–urethane system, *Polymer*, 2006, **47**, 4172–4181, DOI: 10.1016/j.polymer.2006.02.085.

38 P. Majumdar, A. Ekin and D. C. Webster, Thermoset Siloxane-Urethane Fouling Release Coatings, in, *Smart Coatings*, 2007, 61–75, DOI: 10.1021/bk-2007-0957.ch005.

39 P. Majumdar and D. C. Webster, Surface microtopography in siloxane-polyurethane thermosets: The influence of siloxane and extent of reaction, *Polymer*, 2007, **48**, 7499–7509, DOI: 10.1016/j.polymer.2007.10.044.

40 R. F. Brady and I. L. Singer, Mechanical factors favoring release from fouling release coatings, *Biofouling*, 2000, **15**, 73–81, DOI: 10.1080/08927010009386299.

41 M. Berglin and P. Gatenholm, The nature of bioadhesive bonding between barnacles and fouling-release silicone coatings, *J. Adhes. Sci. Technol.*, 1999, **13**, 713–727, DOI: 10.1163/156856199X00956.

42 Z. He, Y. Zhuo, F. Wang, J. He and Z. Zhang, Design and preparation of icephobic PDMS-based coatings by introducing an aqueous lubricating layer and macro-crack initiators at the ice-substrate interface, *Prog. Org. Coat.*, 2020, **147**, 105737, DOI: 10.1016/j.porgcoat.2020.105737.

43 K. Khanafer, A. Duprey, M. Schlicht and R. Berguer, Effects of strain rate, mixing ratio, and stress-strain definition on the mechanical behavior of the polydimethylsiloxane (PDMS) material as related to its biological applications, *Biomed. Microdevices*, 2009, **11**, 503–508, DOI: 10.1007/s10544-008-9256-6.

44 R. N. Palchesko, L. Zhang, Y. Sun and A. W. Feinberg, Development of Polydimethylsiloxane Substrates with Tunable Elastic Modulus to Study Cell Mechanobiology in Muscle and Nerve, *PLoS One*, 2012, **7**(12), e51499, DOI: 10.1371/journal.pone.0051499.

45 R. Moučka and M. Sedlačík, Mechanical properties of bulk Sylgard 184 and its extension with silicone oil, *Sci. Rep.*, 2021, 1–9, DOI: 10.1038/s41598-021-98694-2.

46 A. Dhyani, C. Pike, J. L. Braid, E. Whitney, L. Burnham and A. Tuteja, Facilitating Large-Scale Snow Shedding from In-Field Solar Arrays using Icephobic Surfaces with Low-Interfacial Toughness, *Adv. Mater. Technol.*, 2022, **7**, 1–9, DOI: 10.1002/admt.202101032.

47 Y. Yu, L. Chen, D. Weng, Y. Hou, Z. Pang, Z. Zhan and J. Wang, Effect of Doping SiO 2 Nanoparticles and Phenylmethyl Silicone Oil on the Large-Scale Deicing Property of PDMS Coatings, *ACS Appl. Mater. Interfaces*, 2022, **14**, 48250–48261, DOI: 10.1021/acsami.2c13650.